Active Tab, a New Active Technique for Helicopter Noise Reduction

Kobiki Noboru
Natsuki Kondo
Shigeru Saito

National Aerospace Laboratory of Japan
Chofu, Tokyo, Japan

Takeshi Akasaka
Yasutada Tanabe

Kawada Industries, Inc.
Hagamachi, Tochigi, Japan

Abstract

This paper presents the concept of the active tab which is a new active technique for the helicopter noise reduction, the policy for its aerodynamic design and the results of the experimental activities performed in 2D configuration to evaluate the effect of the active tab with regard to the potential for the noise reduction.

The static wind tunnel test was performed in 2002 to study whether a realistic size tab has the aerodynamic capability equivalent to the noise reduction. It is shown by the test result that the tab of around 8% blade chord with more than 6deg. deflection can achieve the sufficient aerodynamic work for the rotor noise reduction.

The dynamic wind tunnel test was carried out in 2003 to study the unsteady aerodynamic effect of the active tab and to conclude that the more than 11%c active tab extension with 10deg deflection has the sufficient capability for the rotor noise reduction.

Finally, the outline of the future work of this research activity is described.

Introduction

The several active techniques for the helicopter noise and vibration reduction, such as HHC (Higher Harmonic Control) (Refs.1-3), IBC (Individual Blade Control) (Refs.4-6), active flap (Refs.7, 8), active twist (Refs.9, 10) and the like have been proposed, researched and developed so far. Some of them were flight-tested and others are in the phase just close to flight test evaluation. The outlines of each existing active technique, for example on 2 bladed rotor, are depicted schematically in Fig.1.

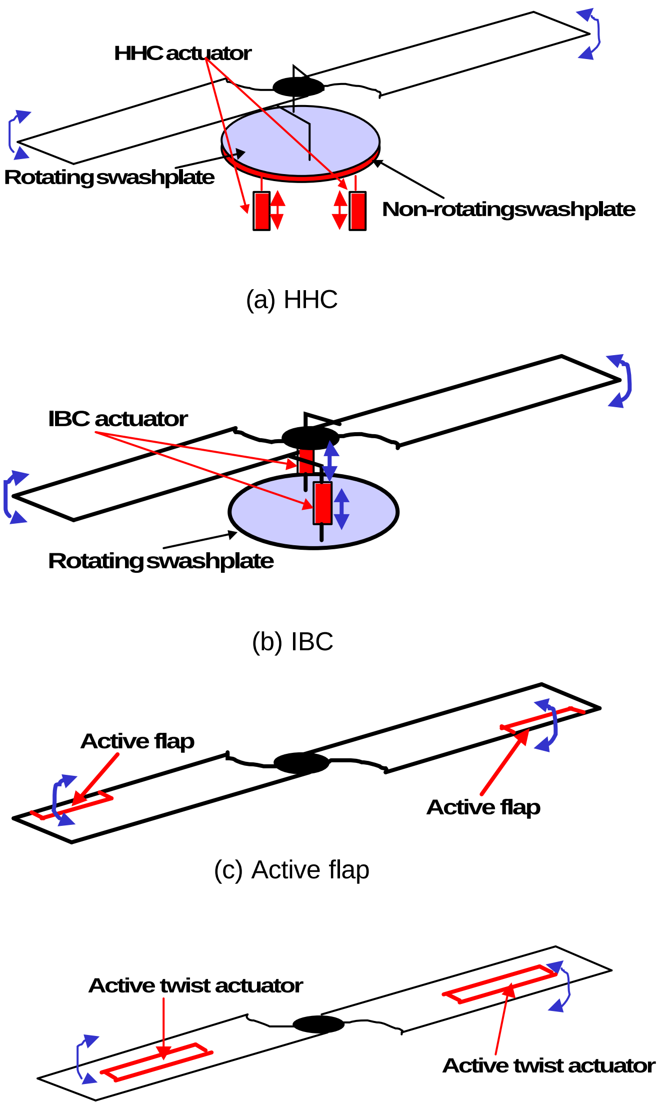

(a) HHC

(b) IBC

(c) Active flap

(d) Active twist

Fig.1 Existing active techniques

HHC shown in Fig.1 (a) actuates the whole blade by the actuator on the non-rotating frame.

This technique has two drawbacks. One is that the actuator is required for high power to drive the non-rotating/rotating swashplates and the inboard portion of the blade as well which are aeroacoustically idle parts. The other is that the higher harmonic pitch frequency able to be appeared on the rotating blade is limited to $b\Omega$ and $(b\pm1)\Omega$, where b and Ω stand for the number of the blades and the rotor speed, respectively.

IBC shown in Fig.1 (b) drives still the whole blade but by the actuator installed on the rotating frame. This technique improves the former drawback of HHC largely and the latter completely at the price of complicated hydraulic system which transmits actuation fluid with high pressure and large flow rate from the non-rotating frame to the rotating frame.

Active flap drives a small flap installed at the trailing edge of a blade tip portion as shown in Fig.1 (c). This technique is power effective compared with HHC and IBC, because only the aeroacoustically useful blade tip part is driven. The flap is actuated by an on-board smart actuator. This technique is materialized by a recent breakthrough in the smart actuator technology area, although the flap drive system still has the challenges in a mechanical component to make enough large flap amplitude with high frequency in high centrifugal force circumstance.

Active twist shown in Fig.1 (d) twists a blade directly by an actuator sheet placed along the blade span underneath the skin without any mechanical component standing between actuator and blade, which makes this technique the best power effective among the four mentioned so far. It is supposed that the effort to generate enough large blade tip amplitude for rotor noise reduction is going on.

In noise reduction respect, these existing active techniques are efficient for BVI (Blade/Vortex Interaction) noise which is generated during the approach to the landing area and occupies a large part of an issue for the public acceptance of helicopter. But these techniques are either not so useful or not so efficient for the noise reduction during climb and fly-over flight patterns as for approach flight pattern.

National Aerospace Laboratory (NAL) and Kawada Industries Inc. have been working together under the joint research program to study and develop a new active technique for helicopter noise reduction which is available to all the three flight patterns in order to cope with this problem. This new technique is named “Active Tab”, which is installed at the airfoil trailing edge of the blade tip portion and is driven back and forth to control the blade lift dynamically.

This paper presents the idea and the wind tunnel testing activity to evaluate the active tab effect as the first step of its research and development.

Objectives

The objectives of this study are as follows;

(1) The fundamental study for the effect of the active tab by 2D static wind tunnel testing.

(2) The unsteady aerodynamic effect of the active tab by 2D dynamic wind tunnel testing.

(3) The feasibility validation of the active tab by these quantitative evaluations.

Description of Active Tab

The concept of the active tab is shown in Fig.2. The active tab is installed at the airfoil trailing edge of the blade tip portion and driven back and forth dynamically to reduce BVI noise and the vibration by the blade lift control due to the variable blade area effect.

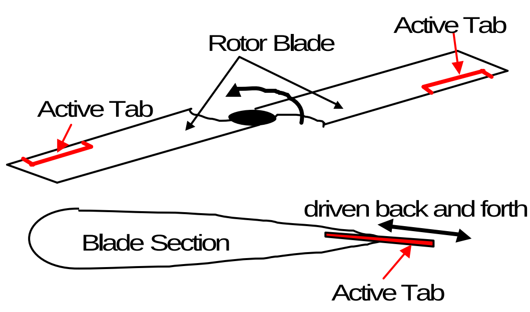

Fig.2 Active tab concept

The active tab also can be operated statically, such as the active tab is deployed with some displacement and fixed. This way of operation can increase the blade lift during the whole revolution of the blade and the rotor speed can be reduced by making use of this surplus lift, which has the noise reduction effect on the climb and fly-over flight patterns.

Criteria for aerodynamic design of active tab

In order to set-up a standard to evaluate the aerodynamic performance of the active tab to possess the sufficient rotor noise reduction capability by the wind tunnel testings without acoustic measurement, the aerodynamic design targets and their reasoning are made as follows.

(1) Controllability for the blade section lift coefficient: more than 0.3;
The rotor blade tip pitch change followed by temporal variation of blade section lift in the blade tip region has a heavy influence to the BVI noise reduction capability, because the blade pitch variation changes the downwash strength, then the miss distance between the tip vortex radiated from the blades and the interfered blade. (Ref.11)
Based on the several previous experimental works which were done for the study of HHC on the BVI noise reduction (Refs.11 and 12), it is indicated that the blade tip deflections in torsion direction with HHC on in case of HHC being effective on the BVI noise reduction had in the order of 3deg amplitude. Assuming the lift curve slope of generic airfoils is 0.1/deg, it is inferred that the controllability of HHC for the blade section lift coefficient of the tip region is conservatively estimated as 0.3.

(2) Active tab chord length: 8 to 15%c;
This is determined by the empirical blade structural restriction and the actuation power limit consideration. Smaller active tab chord than that imposes the significant difficulty on the drive mechanism installation in a thin portion near the trailing edge of the blade and larger one requires much power for the active tab drive actuator.

Wind Tunnel Testings

2D static wind tunnel test

This wind tunnel test was performed to study the fundamental effect of the active tab by 2D static configuration in the 2m by 2.5m low speed wind tunnel of Kawada Industries Inc. as shown in Fig.3.

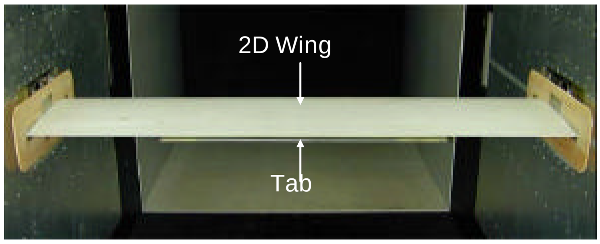

Fig.3 Test set-up (rear view)

Model description The main features of the wind tunnel model are shown in Table 1.

Table 1 Feature of static wind tunnel model

2D wing	Tab
Airfoil: NACA0012	Span: 6, 12, 25, 50, 100%b
Span : 1.62m(b)	Chord: 2.5, 5,10, 15% c
Chord: 0.4m(c)	Deflection: 0, 3, 6deg.

The 2D wing has the end plates on both sides to alleviate the aerodynamic interference of the tunnel wall boundary layer.

The aft portion of the 2D wing is shown in Fig.4, where the tab is installed. The tab part is exchangeable so that a variety of tab geometry such as chord, span and deflection as shown in Table 1 can be studied. The tab parts are glued on the lower side of the 2D wing at the trailing edge as shown in Fig.4.

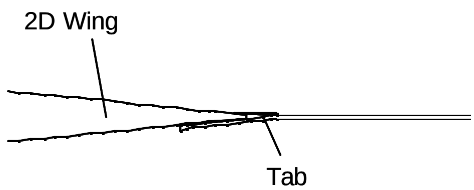

Fig.4 Tab installation

Test condition The wind tunnel test was conducted on the conditions as below.

Wind tunnel speed: 20m/sec
Test section: closed
2D wing angle of attack: -17 to +17deg

Data acquisition/procession The lift, drag and moment are measured by two 3-component balances which support the 2D wing on its both ends at the mid chord location just outside of the wind tunnel walls.

The analog signals coming from the balances are sampled at the rate of 100Hz for 2 sec., then time-averaged to be reduced to the steady aerodynamic coefficients representing the each test case. The moment coefficient is transformed with respect to 1/4 chord position of the 2D wing.

The wind tunnel boundary correction is based on the method described in Ref.13.

2D dynamic wind tunnel test

When it comes to unsteady, the amplitude of the blade lift induced by the active tab may have some difference from that obtained from steady state and the phase shift between the active tab motion and dynamic lift variation may occur.

In order to examine the unsteady aerodynamic effect during the active tab operation, this test was performed in the 2m by 2.5m low speed wind tunnel of Kawada Industries Inc. The sizing and the control parameter such as tab chord, tab deflection, frequency and amplitude were evaluated for the future research activity of the active tab in the rotor configuration.

Model description The main features of the model are shown in Table 2. Fig.5 shows a testing set-up with a fully deployed active tab in the mid span portion of the 2D wing in the wind tunnel.

Table 2 Feature of dynamic wind tunnel model

2D wing	Active tab
Airfoil: NACA0012	Span: 0.2m
Span: 1.62m(b)	Amplitude: 2.5,5,7.5,10%c
Chord: 0.4m(c)	Frequency: 0 to 40Hz
Pressure port position: 0%c and 2,6,11,17,24,42,60,85%c on upper and lower surfaces	

The active tab is operated by a drive mechanism which consists of a DC motor, gear-crank component and a push-pull rod. The rotary motion from the DC motor transmitted to the gear train and transformed into a reciprocating motion, then the back and forth active tab motion is generated via the push-pull rod. The active tab frequency is governed by the DC motor rpm and the active tab amplitude is pre-set at 4 values described in Table 2 by changing the active tab and the connection point of the push-pull rod on the last stage gear.

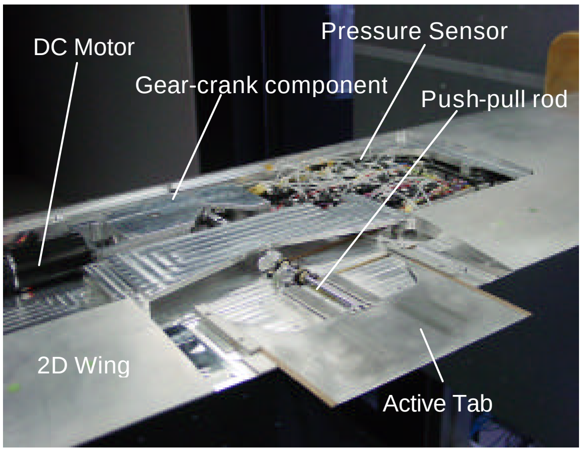

Fig.5 Test set-up (upper rear view)

There are two types of the active tab profile studied in the wind tunnel test. One is the flat tab for which the variable blade area effect is evaluated. The other is the tip bent tab for which the tab deflection effect is examined. Their geometries and motion patterns are depicted in Fig.6 and Table 3.

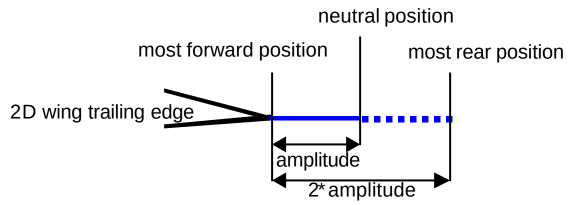

(a) Flat tab

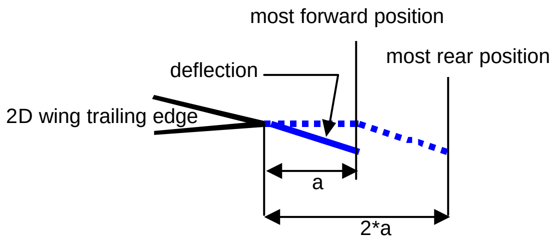

(b) Tip bent tab 1 and 2

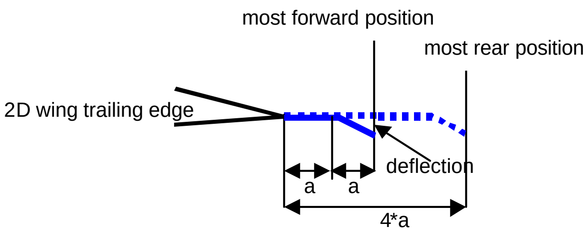

(c) Tip bent tab 3 and 4

Fig.6 Geometry and motion pattern of active tab

Table 3 Geometry of tip bent tab

Active tab	a	deflection
Tip bent tab 1	0.02m	5deg
Tip bent tab 2	0.02m	10deg
Tip bent tab 3	0.01m	5deg
Tip bent tab 4	0.01m	10deg

Test condition The test condition of the dynamic wind tunnel test is shown in Table 4.

Table 4 Test condition of dynamic wind tunnel test

2D wing angle of attack (deg)	Wind tunnel speed (m/s)	Active Tab frequency (Hz)
3	20	2, 5, 10, 20 30, 40Hz
	40	
6	20	
	40	
9	20	
12	20	

Test section: closed

In case of the lower 2D wing angles of attack 3 and 6deg, the test was conducted at the wind tunnel speed of 20 and 40m/s. But in case of the higher 2D wing angles of attack 9 and 12deg, the wind tunnel speed is limited to 20m/s because of the balance capacity. The nominal frequency of the active tab is in the range of 2 to 40Hz, however, the maximum frequency for each active tab is limited case by case because of the capability of the drive power.

Although the reduced frequency of the assumed full scale helicopter in case of active tab application is about 0.15 (equivalent to 4/rev), the wind tunnel testing covers much higher range of the reduced frequency to study the active tab aerodynamic characteristics.

Data acquisition Fig.7 shows the schematic view of the data acquisition. The unsteady aerodynamic force is measured by the balances on both ends of the 2D wing and the chordwise pressure distribution by the 17 pressure transducers disposed along the mid span location from the leading edge to 85%c position of the 2D wing. The active tab displacement is measured by a laser displacement sensor set inside the 2D wing in the vicinity of the active tab drive mechanism. These aerodynamic data and the active tab displacement are acquired simultaneously at the rate of 128 to 2,560Hz depending on the active tab frequency.

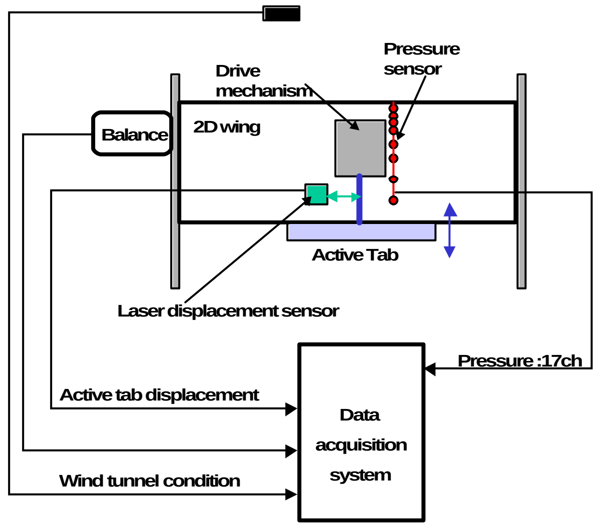

Fig.7 Data acquisition

Data procession The test cases are classified from the data procession point of view into the following three categories as; 1) weight correction case with neither the wind nor the active tab operation, 2) inertia correction case with the active tab operation and without the wind and 3) test run with both the wind and the active tab operation. Each test run is represented by the subtraction between 3) from 1) or 2) on the time history basis, then ensemble averaged with respect to the tab displacement position for fourteen cycles of the tab motion.

In order to correct the finite active tab span 0.2m while 2D wing span is 1.62m and to express the active tab effect as in 2D property, the lift increment coefficient by active tab(Cl) is defined in this work as follows;

$$Cl = (Cl_{with\ active\ tab} - Cl_{without\ active\ tab})*8.1,$$

where a multiplier 8.1 is the ratio of the active tab span to the 2D wing span.

Results and discussion

Static test

Fig.8 shows the lift characteristics with respect to angle of attack with tab chord length and tab deflection as parameters. It can be clearly seen both the chord length and the deflection effects from the baseline which has no tab at the trailing edge.

The difference between the baseline and

the 15%c tab without the deflection comes from the lift curve slope increase due to the enlarged chord length by the tab installation. Approximately 15% increase in the lift curve slope due to 15% increase in the chord length can be seen in Fig.8.

The other difference between the 15%c tab with 6deg deflection and without the deflection indicates the camber effect due to the tab deflection. It can be seen that the lift coefficient increase averagely by 0.3 between near the positive and negative stall angles of attack, which is consistent with that calculated based on the thin airfoil theory.

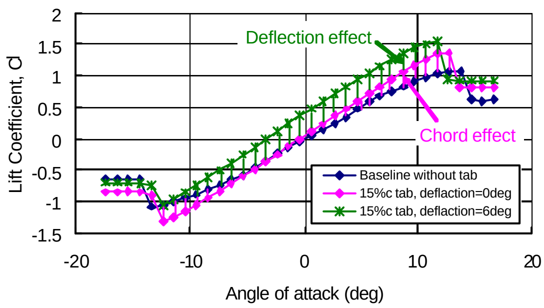

Fig.8 Tab effects on lift characteristics
Wind tunnel speed=20m/sec, Tab span=100%b

Fig.9 shows the tab effect on the drag characteristics in the polar form on the same condition as Fig.8. It is shown that there is no significant drag penalty by the 15%c tab with/without deflection while producing the lift increment in the regular lift range up to 1.0.

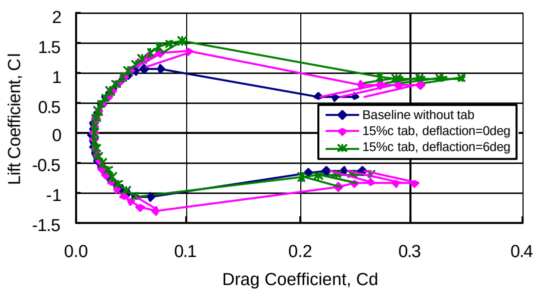

Fig.9 Tab effects on drag characteristics
Wind tunnel speed=20m/sec, Tab span=100%b

Fig.10 shows the tab effect on the moment characteristics on the same condition as Fig.8 and 9. It is shown that there is a compatible influence with that on the lift characteristics, i.e., the effects of enlarged chord length/deflection at the trailing edge generate nose-down moment along with the lift increment.

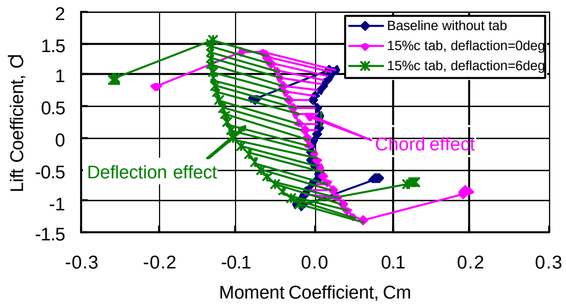

Fig.10 Tab effects on moment characteristics
Wind tunnel speed=20m/sec, Tab span=100%b

Fig.11 shows the tab span effect on the lift characteristics expressed in the term of lift increment ratio which stands for the lift increment of each tab span from the baseline which has no tab normalized by the lift increment of 100%b tab span. It is shown in Fig.11 that the lift increment ratio has linearity with respect to the tab span up to 25%b, however, the 50%b span has a higher lift increment, which is inferred to be caused by the change in the induced angle of attack trend imposed by downwash from the vortices emanated at the both ends of the tab.

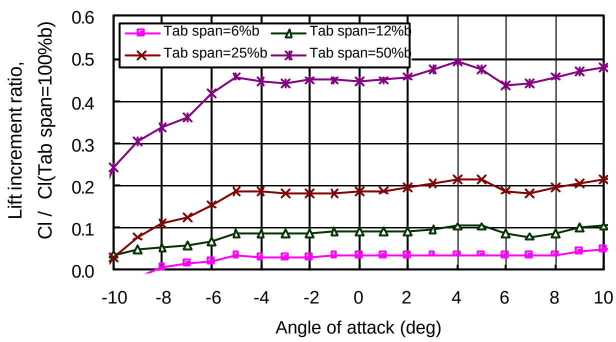

Fig.11 Tab span effect on lift characteristics
Wind tunnel speed=20m/sec, Tab chord=10%c, Tab deflection=6deg

Summarizing the static test results, the domain required for the active tab capable for the noise reduction with the structural restriction is mapped in Fig.12.

The design policy mentioned above is repeated here;
Controllability for the blade section lift coefficient: more than 0.3
Active tab chord length: 8 to 15%c.

Fig.12 shows that these requirements are satisfied by the active tab with 6deg deflection in case of its chord length more than 8%c.

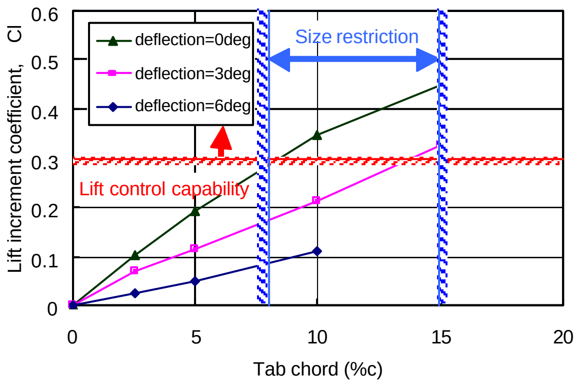

Fig.12 Lift control capability of active tab by static wind tunnel test

Wind tunnel speed=20m/sec, Tab span=100%b

Dynamic test

As mentioned above, the raw time history over the fourteen cycles is averaged with respect to the tab position in order to generate representative time history for each test run case.

Fig.13 shows the validation check of the ensemble averaging of the time history data, for example the whole lift of 2D wing including the lift acting on the active tab, where the ensemble averaged active tab displacement (Fig.13 (a)), the raw time history (Fig.13 (b)) and the ensemble average with data scatter (Fig.13 (c)) are compared together. The tab azimuth used in Fig.13 as a variable of abscissa is defined in such a way that the tab azimuth is equal to 0deg at a full extended active tab position and is equal to 180deg at a fully stored active tab position.

It is shown in Fig.13 that the lift characteristics are consistent with the active tab motion where the larger tab extension makes the larger 2D wing lift value and that the ensemble averaged lift well represents the raw time history with reasonably small data scatter.

Although the active tab performs in a sinusoidal wave form motion as shown in Fig.13 (a), both of the lift time histories shown in Fig.13 (b) and (c) have a bucket shaped aerodynamic free play at around the tab azimuth=180deg and a plateau at around the tab azimuth=0deg. It is found by the data inspection that this phenomenon comes from the difference in the phase between the inertia correction case and the test run case which are described as above.

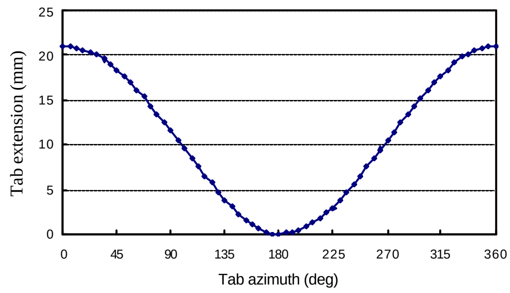

(a) Ensemble average of active tab displacement

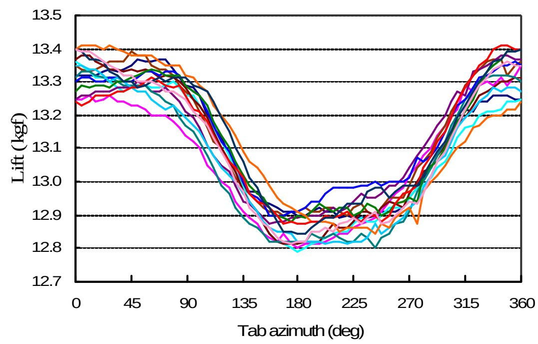

(b) Raw time history of Cl

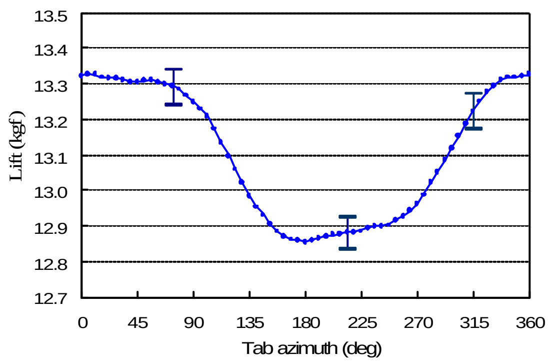

(c) Ensemble average of Cl

Fig.13 Validation of ensemble averaging

Wind tunnel speed=20m/sec,
2D wind angle of attack=9deg,
Active tab frequency=30Hz,
Active tab amplitude=2.5%c

Fig.14 and 15 show the dynamic lift characteristics of the flat tabs and the tip bent tabs, respectively. As mentioned above, Cl is defined as the lift increment by active tab from the baseline without active tab. The phase shift is defined as the delay of the lift time history from the active tab motion at each active tab frequency.

For the flat tabs as shown in Fig.14, the active tab amplitude has a linear effect on the lift increment. The lift increment slightly becomes

larger as the active tab frequency increases.
This is because the 2D wing has a symptom of resonance at higher active tab frequency range induced by the active tab actuation. The phase shift is almost invariant with the active tab amplitude, but has the same tendency as the lift increment, i.e., being larger as the active tab frequency grows. The absolute value of the phase shift is around 200deg, although that should be nearly zero based on the lift increment characteristics. This comes from the difficulty in data processing to identify the real phase shift as mentioned as to Fig.13.

For the tip bent tabs as shown in Fig.15, the effect on the lift increment is clearly seen according to the active tab geometry described in Fig.6 and Table 3. It is shown in this figure that the larger deflected area and deflection makes the larger lift increment in order as tip bent tab 2> tip bent tab 1> tip bent tab 4> tip bent tab 3.

The lift increment slightly becomes larger as the active tab frequency increases, which is also seen in case of the flat tabs by the same reason. As to the phase shift, the similar phenomena to the flat tabs are observed as well.

Fig.16 shows the lift control capability of the active tab obtained by the dynamic wind tunnel test in the same form as that in the static wind tunnel test shown in Fig.12.

Although the limited number of the data points are available in this figure because of the hardware limitation and there can be seen the non-linear lift increment dependency on the active tab amplitude, it is surmised that the requirement is satisfied by the active tab with 10deg deflection in case of its amplitude more than 11%c based on the data trend of the flat tab without deflection.
There is a discrepancy in the required tab geometry to achieve the criteria for aerodynamic design of the active tab between from the static wind tunnel test and from the dynamic one, i.e.,

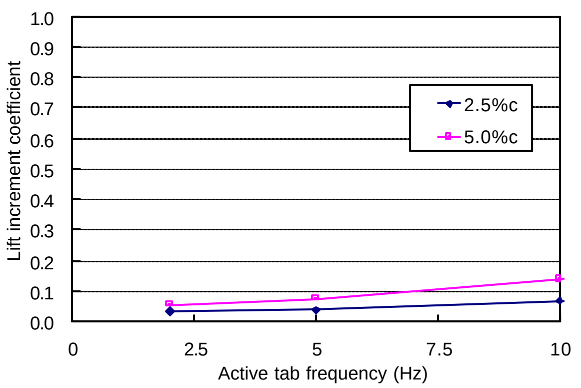

(a) Lift increment coefficient Cl

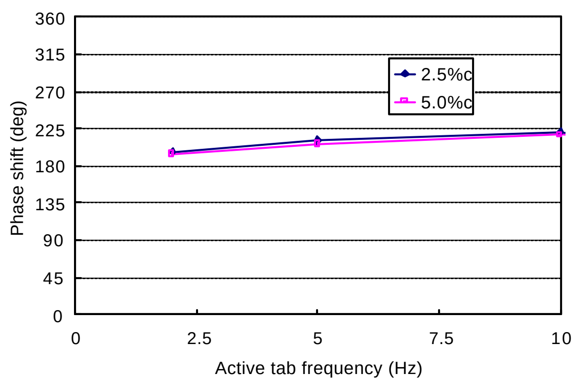

(b) Phase shift

Fig. 14 Dynamic effect on lift by flat tab

Wind tunnel speed=20m/sec,
2D wind angle of attack=9deg

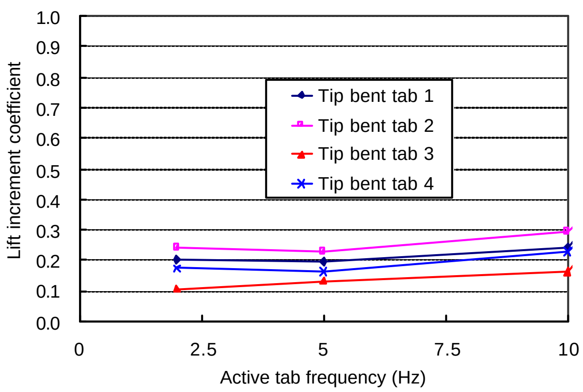

(a) Lift increment coefficient Cl

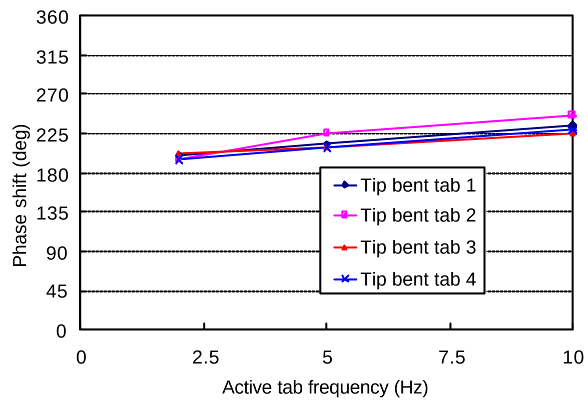

(b) Phase shift

Fig.15 Dynamic effect on lift by tip bent tab

Wind tunnel speed=20m/sec,
2D wind angle of attack=9deg

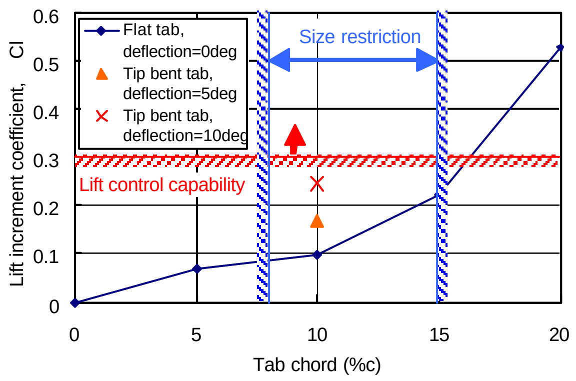

Fig.16 Lift control capability of active tab by dynamic wind tunnel test

Wind tunnel speed=20m/sec,
Tab span=0.2m (1/8b)

8%c extension with 6deg deflection from the static wind tunnel test and 11%c extension with 10deg deflection from the dynamic wind tunnel test. This difference comes from that the tab with deflection used in the static wind tunnel test is fully deflected while the tip bent tabs in the dynamic wind tunnel test is partly deflected as described in Fig.6 and Table 3.

Conclusions

The static and dynamic aerodynamic effects of the active tab were examined by the wind tunnel tests in 2D configuration. Summarizing the experimental results, the followings are concluded by this study.

1. It is shown by the static wind tunnel test that the tab with more than 8% blade chord and 6deg deflection can satisfies the design criteria under which the active can achieve the sufficient aerodynamic work for the rotor noise reduction.

2. It is inferred from the dynamic wind tunnel test that the design criteria is satisfied by the active tab with 10deg deflection in case of its chord length being more than 11%c based on the data trend of the flat tab without deflection.

3. Although there is a discrepancy in the required tab geometry to achieve the criteria for aerodynamic design of the active tab between from the static wind tunnel test and from the dynamic one because of the difference in the tab geometries used in those wind tunnel tests, it is shown that the realistic size of the active tab has the sufficient aerodynamic capability with regard to the lift control which is connected with the potential for the rotor noise reduction.

Future works

So far, the static and dynamic aerodynamic effects of the active tab have been studied by the wind tunnel tests in 2D configuration as described above. The next step is to proceed to 3D rotor configuration where the active tab is installed in a blade of a 1-bladed rotor model to evaluate the active tab effect for the rotor noise reduction and the rotor performance. The efforts for the preparation are now under way.

Acknowledgements

The authors wish to express their thanks to Mr. Kuwako and Mr. Shigeno of Tokai University for their elaboration for data processing presented in this paper.

References

1. Gmelin, B., Heller, H., Philippe, J.J., Mercker, E., Preisser, J.S., “HHC Aeroacoustics Rotor Test at the DNW: The Joint German/French/US HART Project”, 20th European Rotorcraft Forum, Amsterdam, The Netherlands, October 1994, Paper 115.

2. Gmelin, B.L., Heller, H., Mercker, E., Philippe, J.J., Preisser, J.S., Yu, Y.H., "The HART Programme : A Quadrilateral Cooperative Research Effort", 51st Annual Forum of the American Helicopter Society, FortWorth,TX,May 1995, pp 695-709.

3. Murashige, A., Kobiki, N., Tsuchihashi, A., Tsujiuchi, T., Inagaki, K., Yamakawa, E., “Final Report of ATIC Model Rotor Test at DNW”, 57th Annual Forum of American Helicopter Society, Washington D.C., May 9-11, 2001.

4. Jacklin, S., Blaas, A.,Teves, D., Kube, R., “Reduction of Helicopter BVI Noise, Vibration, and Power Consumption Through Individual Blade Control”, 51st Annual Forum of

American Helicopter Society, Fort Worth, Texas, May 9-11, 1995.

5. Haber, A., Jacklin, S., Simone, G., "Development, Manufacturing, and Component Testing of an Individual Blade Control System for a UH-60Helicopter Rotor", American Helicopter Society Aerodynamics, Acoustics, and Test and Evaluation Specialists Meeting, San Francisco, CA, January 23-25, 2002.

6. Jacklin, S., Haber, A., Simone, G., Norman, T., Kitaplioglu, C., Shinoda, P., "Full-Scale Wind Tunnel Test of an Individual Blade Control System for a UH-60 Helicopter", 58th Annual Forum of American Helicopter Society, Montréal, Canada, June 11-13, 2002.

7. Hasegawa, Y., Katayama, N., Kobiki, N., Nakasato, E., Yamakawa, E., Okawa, H., "Experimental and Analytical Results of Whirl Tower Test of ATIC Full Scale Rotor System", 57th Annual Forum of American Helicopter Society, Washington D.C., May 9-11, 2001.

8. Enenkl, B., Klöppel, V., Preißler, D., "Full Scale Rotor with Piezoelectric Actuated Blade Flaps", 28th European Rotorcraft Forum, Bristol, United Kingdom, September 17-19, 2002.

9. Wilbur, L., Mirick, H., Yeager, T., Langston, W., Cesnik, E., Shin, S., "Vibratory Loads Reduction Testing of the NASA/Army/MIT Active Twist Rotor", Journal of the American Helicopter Society, Vol.47, No.2, April 2002, pp.123-133.

10. Bernhard, A., Wong, J., "Sikorsky Active Rotor Control Evaluation of NASA/Army/MIT Active Twist Rotor", 59th Annual Forum of American Helicopter Society, Phoenix, Arizona, May 6-8, 2003.

11. van der Wall, B., "Simulation of HHC on Helicopter Rotor BVI Noise Emission using a Prescribed Wake Method", 26th European Rotorcraft Forum, Den Haag, The Netherlands, September, 2000.

12. Kobiki, N., Murashige, A., "A Study on Blade Torsion Characteristics -Comparison and Evaluation of Analysis with DNW Test Results– ", Heli Japan 2002, Tochigi, Japan, November 11-13, 2002.

13. Rae, W., Pope, A., "Low-Speed Wind Tunnel Testing", John Wiley & Sons, Inc., 1984.